

## EFFECTS OF GRIDS IN DRIFT TUBES\*

M. Okamura<sup>#</sup>, BNL, Upton, NY 11973, USA  
H. Yamauchi, TIME Co., Hiroshima, Japan

### Abstract

In 2011, we upgraded a 201 MHz buncher in the proton injector for the alternating gradient synchrotron (AGS) – relativistic heavy ion collider (RHIC) complex. In the buncher we installed four grids made of tungsten to improve the transit time factor. The grid installed drift tubes have 32 mm of inner diameter and the each grid consists of four quadrants. The quadrants were cut out precisely from 1mm thick tungsten plates by a computerized numerically controlled (CNC) wire cutting electrical discharge machining (EDM). The 3D electric field of the grid was simulated.

### BACKGROUND

In 2010, we modified a 750 keV medium energy beam transport (MEBT) line of proton injector of AGS RHIC complex in Brookhaven National Laboratory (BNL)[1,2]. The MEBT has four quadrupole magnets, four steering and the buncher within 700 mm where is between the radio frequency quadrupole (RFQ) and drift tube linear accelerator (DTL). The installed buncher in 2010 had a half wavelength  $\pi$  mode resonant structure and was machined from a single aluminum block. The inner surface was treated by Alocrom 1000 and the treatment worked well to suppress the secondary electron emission efficiency. The buncher was driven by a 5 kW of RF power amplifier, however the beam transmission measurement indicated that more RF voltage of the buncher might improve the longitudinal matching condition between the RFQ and DTL. Then we built and installed a new high Q copper made buncher to gain a better effective shunt impedance with a newly designed grids. The buncher has two gaps and four grids were installed. The grids help to improve the transit time factor (TTF), however they introduce non-linear field. In this report, we describe simple two-dimensional (2D) analysis results based on a three-dimensional (3D) field simulation. Due to the change of the material, the loaded Q value of the buncher was improved from 2120 to 3600 and the shunt impedance reached 2.0 M $\Omega$ . The installed buncher at the MEBT section is shown at Fig. 1.



Figure 1: The new copper buncher.

\*Work supported by US. DOE. <sup>#</sup>okamura@bnl.gov

### MECHANICAL STRUCTURE OF THE GRIDS

Since the grids are exposed to high current proton beams, the material stands for high temperature condition in vacuum. We used tungsten carbide. A photo of the grid is shown at Fig. 2.



Figure 2: The grid.



Figure 3: The grid in a mockup drift tube.

The inner diameter of the surrounding circle is 32 mm which fits to inner surface of the drift tubes. The drift tubes have grooves those are 1 mm depth and 1 mm width to accommodate grids. The grid consists of four quadrants connected by phosphor bronze springs. The each quadrant was machined from single 1mm thickness tungsten plate

by a CNC wire cutting EDM. The width of the grid facing to the beam direction is 0.2 mm. The connection points between the tungsten quadrants and the springs were brazed but one connection point was remained free. At the installation, this remained free connection point makes easier the process. The edge of the free spring snaps into the hollowed edge of the quadrant. Figure 3 shows the installed grid onto a mockup drift tube.

### FIELD SIMULATION

#### Modeling

In the cavity design stage, Micro Wave Studio[3] was used for the RF simulation. To obtain the detailed 3D information, we used TOSCA-OPERA[4] assuming a static electric condition including the fine structures of the grids. Only one gap was analyzed, although the real buncher has two gaps those are apart  $3/2 \beta\lambda$ . The used 3D model is shown in Fig. 4. Generally, the gap field is expressed as a 3D expansion, however, in this report we used 2D Fourier expansion which is built-in the OPERA post processor since the 2D image is sometimes easier to understand the field deformations. The expansion is written as

$$b_0 + \sum_k (a_k \sin k + b_k \cos k) \quad (1)$$

A cylindrical coordinate system is defined as ‘z axis = beam axis.’ So the field components are expressed as  $E_r, E_\theta, E_z$ . The coefficients were derived from the field along the yellow circle indicated in the figure. The radius of the circle is 7 mm from the beam axis which is just inside of the apexes of the grid’s pattern.

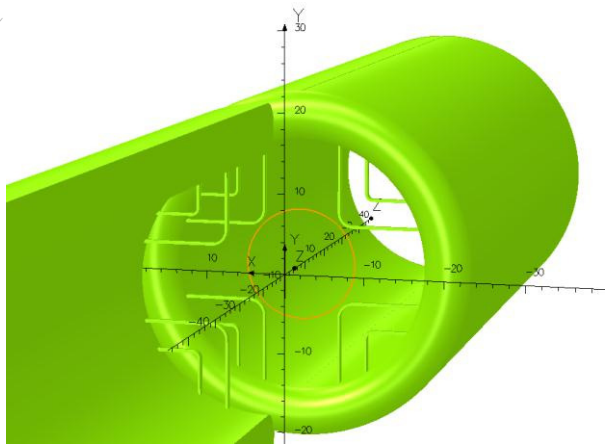


Figure 4: 3D model for OPERA.

The inner diameter and gap length are 32 mm and 10 mm. The edge of the tube are rounded by  $r = 3$  mm and the grid’s face started at  $z = \pm 3.1$  mm position. The distance between two facing grids is 16.2 mm. In this analysis, the gap voltage is assumed as 100 V.

#### Transit Time Factor

Figure 5 shows longitudinal electric field strengths at  $r = 7$  mm,  $b_0$  component of  $E_z$  along the beam axis, with and without grids. The dotted lines include RF phase change assuming a 750 keV proton beam. At  $z = 0$  position, the RF phase of *cosine* is zero. At the tail of the fields, the induced voltage has negative value around  $z = 15$ -30 mm. If the cavity employs  $\beta\lambda/2$  gap interval, these negative effect could be avoided, since the  $\beta\lambda/2 = 30$  mm.

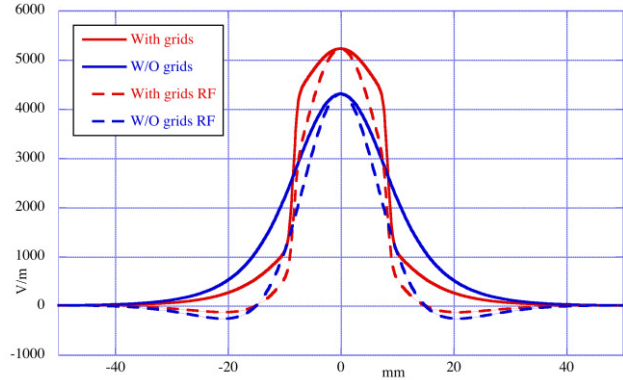


Figure 5: Longitudinal field strength ( $r = 7$ mm).

TTF can be derived by comparing the solid curves and dotted curves at the certain phase (the graph shows zero phase angle). The obtained values are summarized in Table 1.

Table 1: Transit Time Factors

On axis	With grids	63.50 %
	Without grids	50.14 %
$r = 7$ mm	With grids	72.28 %
	Without grids	57.03 %

The grids enhance the TTF about 26 %.

#### Transverse Field

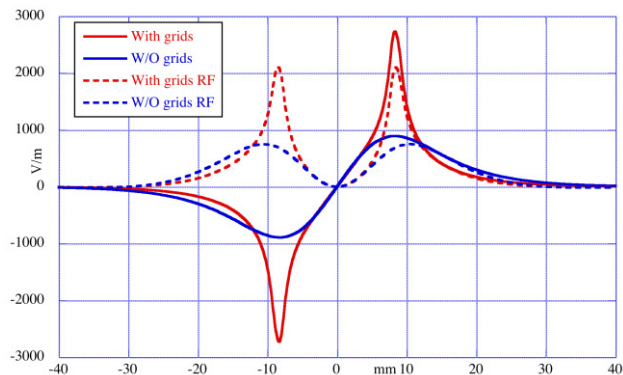


Figure 6: Transverse field strength ( $r = 7$ mm).

$b_0$  component of  $E_r$  represents focusing and defocusing force. Figure 6 shows the component. The dotted lines include the RF phase angle of  $-90^\circ$  at  $z = 0$  position. The integrated values along the axis with grid and without

grids are 24.9 % and 19.7 % of the gap voltage respectively. The grids emphasize the RF defocusing force by choosing a bunching RF phase.

### Multipole Distortions

Due to the presence of the grids, the field has multipole components. Figure 7 shows the higher components of  $E_z$ .

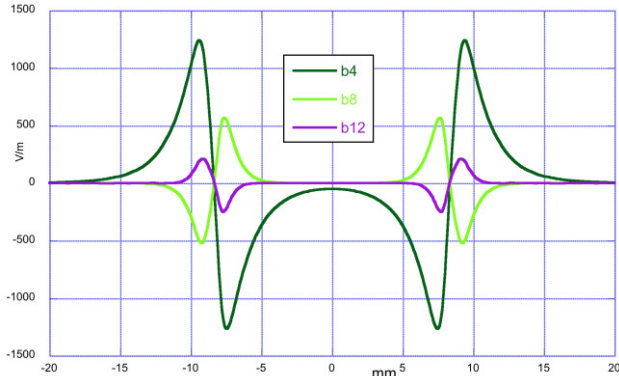


Figure 7: Multipoles of  $E_z$  ( $r = 7$ mm).

Figures 8 and 9 show multipoles of  $E_r$  and  $E_\theta$ . Unfortunately when we select the RF phase angle as  $-90^\circ$  or  $90^\circ$ , these distortions will be maximized.

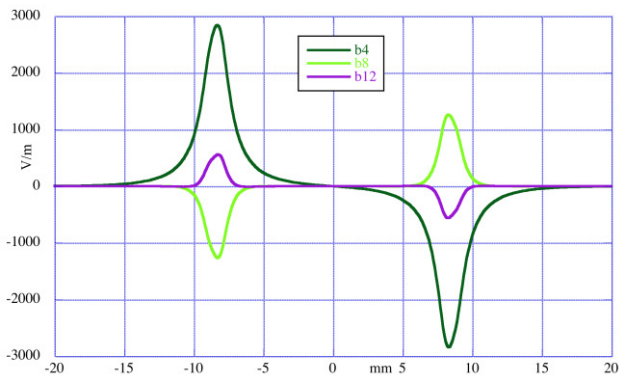


Figure 8: Multipoles of  $E_r$  ( $r = 7$ mm).

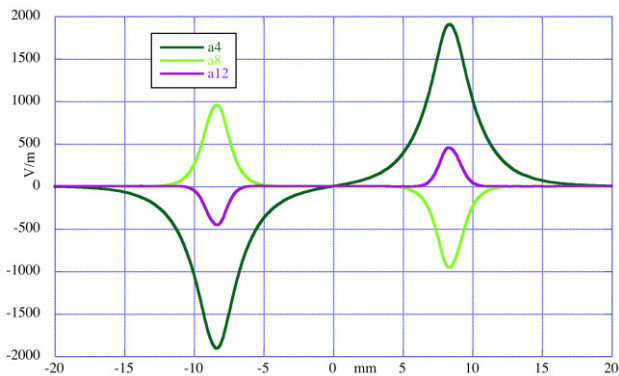


Figure 9: Multipoles of  $E_\theta$  ( $r = 7$ mm).

To investigate the nonlinear effects on a beam, detailed tracking simulation or experimental study is required.

### SUMMARY

We developed a new mechanical structure of grids for the 201 MHz  $3\beta\lambda/2$  buncher for 750 keV proton beam. The grids are quite effective to improve the transit time factor. However, the major multipole components and the RF defocusing force are increased, when it is operated at  $-90^\circ$  of the RF phase.

### ACKNOWLEDGMENT

Authors thank to D. Raparia, J. Fite, V. LoDestro and J. Alessi of Brookhaven National Laboratory, M. Yoshida of Time Corporation and N. Hayashizaki of Tokyo Institute of Technology.

### REFERENCES

- [1] M. Okamura, B. Briscoe, J. Fite, V. LoDestro, D. Raparia, J. Ritter and N. Hayashizaki "A New Medium Energy Beam Transport Line for The Proton Injector of AGS-RHIC," LINAC'10, Tsukuba, September 2010, TUP027, p. 458 (2010); <http://www.JACoW.org>.
- [2] D. Raparia, J. Alessi, J. Fite, O. Gould, V. LoDestro, M. Okamura, J. Ritter and A. Zelenski "Low and Medium Energy Beam Transport Upgrade at BNL 200 MeV LINAC," LINAC'10, Tsukuba, September 2010, TUP026, p. 455 (2010); <http://www.JACoW.org>.
- [3] CST MICROWAVE STUDIO <http://www.cst.com/>
- [4] OPERA-TOSCA, Vector Fields Software, Cobham <http://www.cobham.com>